

Ultrafast Energy Transfer between the $^3\text{MLCT}$ State of $[\text{Ru}^{\text{II}}(\text{dmb})_2(\text{bpy-an})]^{2+}$ and the Covalently Appended Anthracene

Jon R. Schoonover, Dana M. Dattelbaum, Anton Malko, Victor I. Klimov, and Thomas J. Meyer*

Los Alamos National Laboratories, Los Alamos, New Mexico 87545

David J. Styers-Barnett, Erika Z. Gannon, Jeremy C. Granger, W. Steven Aldridge, III, and John M. Papanikolas*

Department of Chemistry, University of North Carolina, Chapel Hill, North Carolina 27599

Received: December 7, 2004

The time scale for triplet–triplet energy transfer (EnT) between a Ru(II) chromophore and a ligand bound anthracene acceptor in $[\text{Ru}^{\text{II}}(\text{dmb})_2(\text{bpy-an})]^{2+}$ (dmb = 4,4'-dimethyl-2,2'-bipyridine; bpy-an = 4-(9-anthrylethylene), 4-methyl-2,2'-bipyridine) has been measured using femtosecond transient absorption spectroscopy. The appearance of the anthracene excited state is monitored following photoexcitation to a metal-to-ligand charge transfer (MLCT) state via the $\pi\pi^*$ absorption of the triplet excited state of anthracene. Our time-resolved experiments show the presence of fast, sub-100 ps energy transfer to the anthracene occurring on two characteristic time scales of 23 and 72 ps.

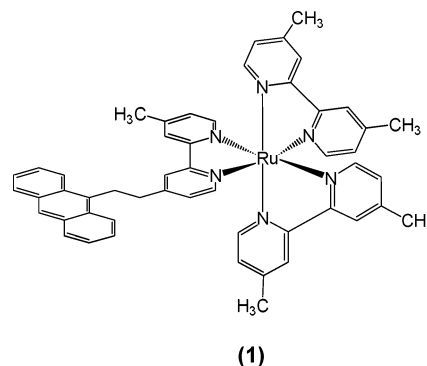
I. Introduction

The combined optical properties and photostability of Ru(II) and Os(II) trispolypyridyl compounds make them attractive building blocks for molecular devices.^{1–6} However, to rationally design molecular architectures based on chromophores that have specific functionalities we must understand in detail how energy and charge flow within molecular building blocks as well as between adjacent components. Time-resolved studies performed in our lab and others indicate that many of the photoinduced processes, including internal conversion (IC), vibrational cooling (VC), interligand electron transfer (ILET), and energy transfer (EnT), happen on similar time scales.^{4–7} These studies have focused on primarily the dynamics within a single photoexcited complex. Our attention now turns to the dynamics of energy transport between covalently attached components. In this paper, we describe femtosecond transient absorption studies of energy transfer between a Ru(II) polypyridyl chromophore with a covalently appended anthracene acceptor.

Energy transfer has been studied between Ru(II) polypyridyl complexes and unbound aromatics, as well as covalently appended aromatics, using steady state and nanosecond time-resolved emission spectroscopies,^{8–16} and several trends have been identified. When naphthalene is the acceptor, energy transfer from the lowest metal-to-ligand charge-transfer triplet ($^3\text{MLCT}$) state¹⁷ is not observed because the aromatic triplet excited state is higher in energy, and thus the luminescence from the $^3\text{MLCT}$ is unaltered. Pyrene's excited state is isoergic with the $^3\text{MLCT}$ state ($\Delta G^\circ \sim 0$) and equilibrium between the two triplet states is established through forward and reverse energy transfer. In this system, the long lifetime of the $^3\pi\pi^*$ state extends the MLCT luminescence lifetime, which can be as long as 145 μs .¹⁴ Anthracene, however, has an excited triplet state that is lower in energy, and therefore $^3\text{MLCT}$ luminescence is quenched via efficient energy transfer.

While energy transfer in these bichromophoric systems has been widely researched, many questions still remain. For

example, although it is known that Ru(II)polypyridyl–anthracene complexes undergo energy transfer with near unit efficiency, both the time scale of this process and its relationship to other excited-state processes (e.g., VC, IC, ILET) are unknown. The experiments presented here use femtosecond transient absorption spectroscopy to measure energy transfer rate constants from the $^3\text{MLCT}$ state of the metal complex to a $^3\pi\pi^*$ state on the anthracene in $[\text{Ru}^{\text{II}}(\text{dmb})_2(\text{bpy-an})]^{2+}$, where dmb = 4,4'-dimethyl,2,2'-bipyridine and bpy-an = 4-(9-anthrylethyl),4'-methyl-2,2'-bipyridine (**1**).



We observe fast, $^3\text{MLCT} \rightarrow \text{An}$ energy transfer that occurs with two characteristic time components of 23 and 72 ps. These components could reflect the presence of two different ground state conformations (e.g., with the An folded in near the bipyridine or with the An extended out at the end of its tether) or the flow of MLCT excitation among the three polypyridyl ligands prior to energy transfer to the anthracene. Regardless of the mechanism, this result does establish that energy transfer is essentially complete on a sub-100 ps time scale with approximately 60% of the total excited-state population transferred to the ligand-bound anthracene in about 70 ps.

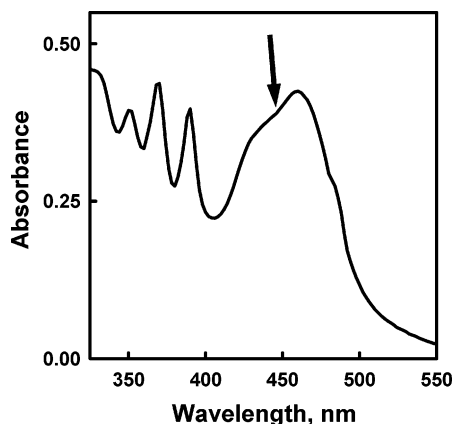


Figure 1. Absorption spectrum of $[\text{Ru}^{\text{II}}(\text{dmb})_2(\text{bpy-an})]^{2+}$. The arrow indicates the excitation wavelength.

II. Experimental Description

The femtosecond transient absorption spectrometer is based on a commercially available ultrafast laser system (Clark CPA-2001) consisting of an erbium-doped fiber ring oscillator and a chirped pulse Ti:sapphire regenerative amplifier that is pumped by a frequency doubled, Q-switched Nd:YAG laser. The amplifier produces 120 fs laser pulses at 775 nm with a 1 kHz repetition rate and a pulse energy of approximately 950 μJ /pulse. The majority of this laser output is sent into an optical parametric amplifier (OPA) to provide tunable femtosecond excitation laser pulses (pump beam). The remainder of the laser output is focused at a CaF_2 window to generate the white light continuum used as the probe beam. Further details of the experimental apparatus have been described elsewhere.⁵ For the experiments presented in this paper, the OPA was tuned to produce 450 nm pump pulses ($\sim 1 \mu\text{J}$ /pulse) focused to a 500 μm spot size and overlapped with the probe beam at the sample. Transient absorption spectra were collected between 350 and 430 nm. The polarization angle between the pump and probe beams was set to the magic angle (54.7°) to eliminate polarization effects in the collected spectra.

The salt of $[\text{Ru}^{\text{II}}(\text{dmb})_2(\text{bpy-an})](\text{PF}_6)_2$ was prepared and characterized as described previously.¹⁸ Dilute solutions were prepared in distilled, dried acetonitrile, placed in a 2 mm path length cuvette, and flowed using a peristaltic pump. All solutions were deoxygenated by sparging with argon for 1 h and were kept under argon for the duration of the spectroscopic measurements. Efforts were made to eliminate all unnecessary light to prevent photodegradation of the sample. Photodegradation occurs as endoperoxide formation across the center ring of the anthracene. This destroys the acceptor and shuts down the pathway for energy transfer in the complex. All experiments were conducted at room temperature (20 $^\circ\text{C}$).

III. Results and Discussion

The ground-state absorption spectrum of $[\text{Ru}(\text{dmb})_2(\text{bpy-an})]^{2+}$ in acetonitrile (Figure 1) exhibits several prominent features. The absorptions between 340 and 400 nm arise from $\pi\pi^*$ transitions of ground-state anthracene, and the broad transition centered at 450 nm arises from the promotion of an electron from a $d\pi$ orbital on the metal center to a π^* orbital on one of the three polypyridyl ligands to form a $^1\text{MLCT}$ state. Bands due to direct excitation to the lowest $^3\text{MLCT}$ states occur in the low energy tail of the absorption spectrum. The MLCT absorption band in the functionalized complex is identical in shape to the spectrum of $[\text{Ru}(\text{dmb})_3]^{2+}$, indicating that the

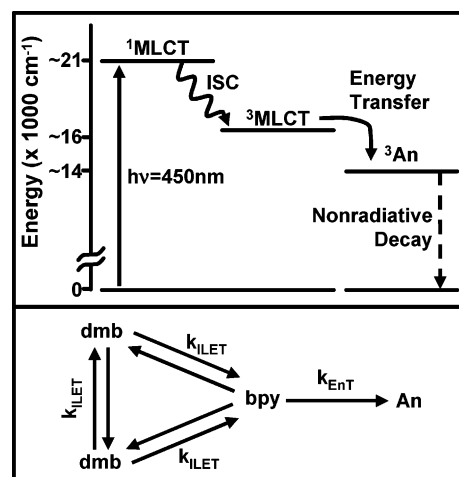


Figure 2. Upper panel: Energy level diagram for $[\text{Ru}^{\text{II}}(\text{dmb})_2(\text{bpy-an})]^{2+}$. Lower panel: Kinetic scheme for interligand electron transfer and energy transfer in the molecule. Initial excitation can occur on any of the polypyridyl ligands (dmb or bpy) with the final fate for excited-state energy on the anthracene (An).

electronic structure of the Ru core is not altered by the presence of the anthracene moiety. Thus, excitation at 450 nm exclusively excites the metal polypyridyl core.

An energy level diagram depicting the dynamic processes that occur in the complex is displayed in the upper portion of Figure 2. Transient absorption studies on $[\text{Ru}^{\text{II}}(\text{bpy})_3]^{2+}$ have shown⁶ that photoexcitation of the $^1\text{MLCT}$ state is followed by relaxation into a manifold of $^3\text{MLCT}$ states within 300 fs. As noted in Figure 2, there are three degenerate (or nearly degenerate) MLCT states. Two are based on the dmb ligand, and one is based on the polypyridyl fragment of the bpy-an ligand.

Because this relaxation takes place within the time resolution of our instrument, the $^3\text{MLCT}$ is the earliest discernible state in these experiments. The driving force for energy transfer¹⁹ from the $^3\text{MLCT}$ state to the lowest $\pi\pi^*$ triplet state of anthracene is 2200 cm^{-1} and is sufficiently rapid that EnT occurs with near unit efficiency. As a result, all luminescence from the Ru(II) core is quenched. The anthracene excited state decays back to the ground state through primarily nonradiative pathways with a lifetime well outside the time scale of these experiments ($\gg 1 \text{ ns}$).¹⁸

Excited state absorption spectra of the Ru-bpy-an complex at a series of times after photoexcitation are shown in Figure 3. At early times, the spectrum shows a broad absorption centered at 370 nm arising from the $^3\text{MLCT}$ states of the $[\text{Ru}^{\text{II}}(\text{dmb})_3]^{2+}$ core. As time evolves this feature decays away and a strong absorption appears at 425 nm. This new band corresponds to the $^3\pi\pi^*$ excited state of anthracene. The isosbestic point at 395 nm is evidence of a simple D \rightarrow A energy transfer process. The kinetics associated with the appearance of the $^3\pi\pi^*$ state are depicted in Figure 3B, which shows that approximately 60% of the total MLCT excited-state population is transferred to the ligand-bound anthracene in about 70 ps.

This time scale is comparable to triplet-triplet energy transfer rates observed between polypyridylmetal complexes and ligand bound acceptors when the two are linked via a conjugated bridge. Castellano et al.¹⁴ have reported $\tau_{\text{EnT}} = 35 \text{ ps}$ in a Ru-(polypyridyl) complex covalently attached to a pyrene molecule through a single bond. Harriman et al.⁹ measured τ_{EnT} for Ru and Os complexes covalently attached to a pyrene molecule through a triple bond, as well as through a Pt spacer. In the conjugated system $\tau_{\text{EnT}} = 7 \text{ ps}$ while the nonconjugated Pt bridge slowed transfer down to the nanosecond time scale. Juris

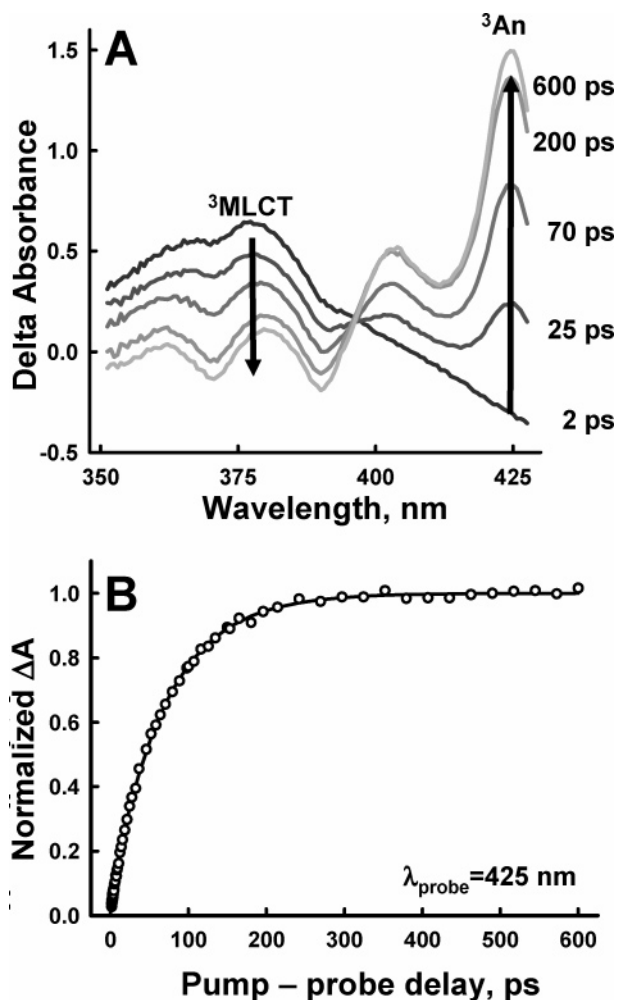


Figure 3. (A) Excited-state absorption spectra at a series of pump–probe delays. Decay of the $^3\text{MLCT}$ absorption at 375 nm corresponds with the growth of the intense ^3An absorption at 425 nm. (B) Transient signal for ^3An excited-state growth. The solid line shows the best-fit results of the model.

and Prodi²⁰ have also measured energy transfer in nonconjugated metal trispyridyl–pyrene supermolecular systems, and found that energy transfer occurs in nanoseconds as well. While the connective bridges in these systems are relatively dissimilar to ours, a general trend of reduced rate constants in nonconjugated systems for triplet energy transfer has been observed elsewhere. Our system exhibits transfer times that resemble the conjugated systems, despite the fact that there is no conjugation present in our bridge. A possible explanation for the fast rate of energy transfer in our complex could be that the ethyl linkage allows adequate mobility for the anthracene to position itself so that the molecular orbitals of the bpy and the anthracene could achieve good electronic communication.

Closer inspection of the absorption transient shows the presence of two time components in the growth of the anthracene excited-state absorption. A nonlinear least-squares fit to a biexponential growth reveals fast and slow components of 23 (10%) and 72 ps (90%), respectively. Biphasic kinetics implies that two pathways to energy transfer exist.

One simple explanation of this biphasic growth behavior is that it stems from two different donor–acceptor ground state conformations due to the flexible coupling between the metal complex and the anthracene. The fast component (23 ps) would then correspond to a geometry with the anthracene folded close to the bipyridine ligand (in), and a slow energy-transfer time

(72 ps) would result when the anthracene was extended away from the metal complex (out). The observed amplitudes (10% and 90%) would then reflect the relative populations of the two states.

A second explanation for this biphasic behavior is that it stems from the flow of MLCT excitation among the three ligands *prior* to energy transfer to the anthracene. Biphasic growth kinetics arise in this model (Figure 2) because photoabsorption has *equal* probability of placing the MLCT excitation on any one of the three ligands, resulting in equal populations on each ligand. Excited states formed on the bpy-an ligand undergo direct energy transfer to the appended anthracene (An) with a rate constant k_{EnT} . MLCT states formed on one of the dmb ligands first require energy migration to the bpy-an ligand (i.e. inter-ligand electron transfer, ILET) *before* energy transfer to the anthracene occurs. The rate of the anthracene excited-state growth observed in the experiment is a superposition of these two pathways.

We have to fit the growth of the anthracene excited state to this kinetic model in order to extract rate constants for ILET, k_{ILET} , and energy transfer, k_{EnT} . In $[\text{Ru}(\text{dmb})_2(\text{bpy-an})]^{2+}$ the polypyridyl fragments of all the ligands are nearly energetically equivalent. The driving force for internal energy transfer from dmb to bpy-an ligand is estimated to be only $\sim 150 \text{ cm}^{-1}$ from electrochemical data. Given the small driving force, we approximate $k_{\text{ILET}} = k_{\text{ILET}}^{-1}$ in the analysis. Following photon absorption, the excited state population, which is initially distributed equally among the three ligands, evolves through ILET and energy transfer until it resides solely on the anthracene. The result of a nonlinear least-squares fit to the model is the solid line in Figure 3B. This analysis yields a lifetime for energy transfer of 16 ps ($k_{\text{EnT}} = 6.25 \times 10^{-14} \text{ s}^{-1}$), and an ILET lifetime of 27 ps ($k_{\text{ILET}} = 3.70 \times 10^{-14} \text{ s}^{-1}$). The latter value is similar to that reported by Malone and Kelley for $\text{Ru}(\text{bpy})_3^{2+}$ (47 ps),²¹ but three times slower than the ILET rate constant measured in our lab for $\text{Os}(\text{bpy})_3^{2+}$ (8.7 ps in acetonitrile).⁵ The slower rate constant for Ru compared to Os is consistent with its lower spin–orbit constant (~ 1000 vs $\sim 3000 \text{ cm}^{-1}$) and a lesser degree of mixing between the nearly degenerate $^3\text{MLCT}$ excited states.

The amplitudes of the fast and slow components of this model are determined by relative magnitudes of k_{ILET} and k_{EnT} . When ILET is fast compared to energy transfer ($k_{\text{ILET}} \gg k_{\text{EnT}}$), the excited state population will off-load slowly to anthracene. Because energy transfer is the rate-limiting step, the fast amplitude will become zero and a single slow component will be observed. On the other hand, when energy transfer is significantly faster than ILET ($k_{\text{EnT}} \gg k_{\text{ILET}}$), one-third of the population will transfer to anthracene promptly, while the other two-thirds will be delayed due to the ILET step. The result is that both fast and slow components will be observed, and their amplitudes will be 33% and 66%, respectively. When the two rates are comparable, a fast component will be observed, but its amplitude will be less than 33% of the total. In this kinetic scheme, the relative amplitudes of the two components are constrained by the magnitudes of the rate constants themselves, and the relative amplitudes that are observed in the experiment are consistent with those predicted by the model given the two time scales. Although this observation does not confirm this energy flow model, it does lend support to its validity. Regardless of the origin of this biphasic behavior, the experiments presented in this publication have identified that energy transfer occurs on a sub-100 ps time scale.

Acknowledgment. Funding for this project was provided by the Petroleum Research Fund (grant 36385-G6), Research Corporation Award RI0048, the National Science Foundation (CHE-0301266), the United States Department of Energy (grant DE-FG02-96ER 14607), Los Alamos National Laboratories' Laboratory Directed Research and Development Program (project 20020222ER), and the University of North Carolina.

References and Notes

- (1) Creutz, C.; Chou, M.; Netzel, T. L.; Okumura, M.; Sutin, N. *J. Am. Chem. Soc.* **1980**, *102*, 1309–1319.
- (2) Meyer, T. J. *Pure Appl. Chem.* **1986**, *58*, 1193.
- (3) Vlcek, A., Jr. *Coord. Chem. Rev.* **2000**, *200–202*, 933–977.
- (4) Damrauer, N. H.; McCusker, J. K. *J. Phys. Chem. A* **1999**, *103*, 8440–8446.
- (5) Shaw, G. B.; Brown, C. L.; Papanikolas, J. M. *J. Phys. Chem. A* **2002**, *106*, 1483–1495.
- (6) Damrauer, N. H.; Cerullo, G.; Yeh, A.; Boussie, T. R.; Shank, C. V.; McCusker, J. K. *Science* **1997**, *275*, 54–57.
- (7) Monat, J. E.; McCusker, J. K. *J. Am. Chem. Soc.* **2000**, *122*, 4092–4097.
- (8) Olmsted, J.; Meyer, T. J. *J. Phys. Chem.* **1987**, *91*, 1649–1655.
- (9) Hissler, M.; Harriman, A.; Khatyr, A.; Ziessel, R. *Chemistry: A Eur. J.* **1999**, *5*, 3366–3381.
- (10) Belsler, P.; Dux, R.; Baak, M.; De Cola, L.; Balzani, V. *Angew. Chem. Int. Ed. Engl.* **1995**, *34*, 595–598.
- (11) Wilson, G. J.; Sasse, W. H. F.; Mau, A. W. H. *Chem. Phys. Lett.* **1996**, *250*, 583–588.
- (12) Simon, J. A.; Curry, S. L.; Schmechl, R. H.; Schatz, T. R.; Piotrowiak, P.; Jin, X.; Thummel, R. P. *J. Am. Chem. Soc.* **1997**, *119*, 11012–11022.
- (13) El-ghayoury, A.; Harriman, A.; Khatyr, A.; Ziessel, R. *J. Phys. Chem. A* **2000**, *104*, 1512–1523.
- (14) Tyson, D. S.; Henbest, K. B.; Bialecki, J.; Castellano, F. N. *J. Phys. Chem. A* **2001**, *105*, 8154–8161.
- (15) McClenaghan, N. D.; Barigelletti, F.; Maubert, B.; Campagna, S. *Chem. Commun.* **2002**, 602–603.
- (16) Maubert, B.; McClenaghan, N. D.; Indelli, M. T.; Campagna, S. *J. Phys. Chem. A* **2003**, *107*, 447–455.
- (17) The lowest ³MLCT state is actually a manifold of three closely spaced states split in the parent triplet by low symmetry and spin–orbit coupling.
- (18) Weinheimer, C.; Choi, Y.; Caldwell, T.; Gresham, P.; Olmsted, J., III *J. Photochem. Photobiol. A: Chemistry* **1994**, *78*, 119–126.
- (19) Aldridge, W. S., III *Design and Synthesis of Chromophore-Quencher Molecular Assemblies*; University of North Carolina, 2000.
- (20) Juris, A.; Prodi, L. *New J. Chem.* **2001**, *25*, 1132–1135.
- (21) Malone, R. A.; Kelley, D. F. *J. Chem. Phys.* **1991**, *95*, 8970–8976.